

EyeSat: a great student adventure within the French space agency leading up to lessons learned from orbit

Fabien Apper, Antoine Ressouche, Nicolas Humeau, Matthieu Vuillemin, Guillaume Crooks, Gregor Vindry
 U-Space
 10 avenue Edouard Belin, 31400 Toulouse, France; +337 88 03 77 68
fabien.apper@u-space.fr

Frédéric Viaud, Nicolas Verdier, Stéphane Fredon, Alain Gaboriaud
 CNES
 18 avenue Edouard Belin, 31400 Toulouse, France; +335 61 27 31 31
nicolas.verdier@cnes.fr

ABSTRACT

EyeSat has been a tremendous, challenging and successful student project. With 250 students over 7 years, CNES has achieved to put in orbit a 3U CubeSat that carries tens of state-of-the art innovative nanosatellite subsystems resulting from R&D programs carried out within the French space ecosystem. Launched in December 18, 2019, EyeSat has proved to be fully functional in orbit and has started its mission to map the intensity and the polarization direction of the zodiacal light. Housekeeping data, acquired over the past 5 months, has been analyzed by the team. Precious comparisons have been made between design and simulation results on the one hand and actual data on the other. Now, the private company U-Space, created in 2018, leverages those lessons learned from EyeSat and provides space missions based on high-performance nanosatellites.

INTRODUCTION

EyeSat is an astronomy and technology demonstration project based on a 3U CubeSat and carried out internally within the French Space Agency (CNES) by students. More than 250 students worked on the project, from phase 0 to in-flight operations.

The project has 3 objectives:

- the training of students in space engineering ;
- the in-orbit demonstration of subsystems developed through CNES R&D : On-Board Computer based on a ARM9 microprocessor, X-band payload telemetry, S-band transceiver, flight software implementing time and space partitioning ;
- the mapping of the intensity and the polarization direction of the zodiacal light in different spectral bands.

The project started in September 2012 and EyeSat was launched on December 18, 2019 by a Soyuz rocket from the French Space Center in Guyana. EyeSat was injected on a Sun-synchronous orbit - local time 6am with an altitude around 500 km.

SATELLITE

The figure below shows EyeSat. The CubeSat's bus is composed of four deployable solar panels, a power board, a magnetorquer board, an S-band transceiver, an on-board computer, an X-band transmitter, an interface board, four reaction wheels, a star tracker, two S-band antennas and one X-band antenna. The payload is a telescope which comprises a color CMOS detector, a two-stage filter wheel, a piece of optics and a baffle. For more details about EyeSat's components, refer to [3].

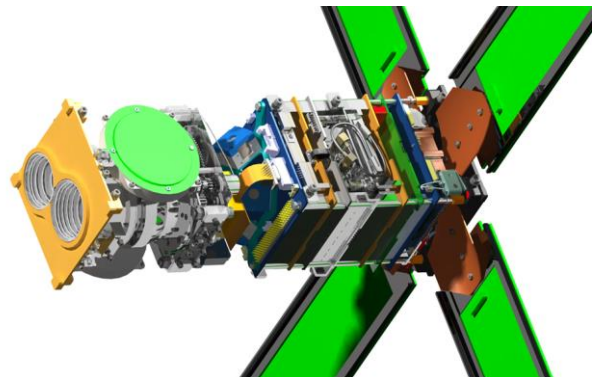


Figure 1: EyeSat CAD model

IN-FLIGHT RESULTS

Operational since December 18, 2019, EyeSat has provided a large amount of in-flight data. The following sections aim at comparing what was expected from what it really is.

Payload

The payload is a small telescope called IRIS composed of 4 elements:

- a baffle designed to suppress stray light with a 40 degrees exclusion angle ;
- a commercially available optic with a 50 mm focal length and a 1.4 aperture giving a 13 degree field of view. This optic has been reworked to be compatible with the space environment ;
- a two-stage filter wheel. The first stage has three filters: black cover, visible light, near infrared light. The second stage has four filters: no polarization and three polarizing filters ;
- a detector based on a CMOS sensor consisting of a 2048*2048 pixel bayer matrix.

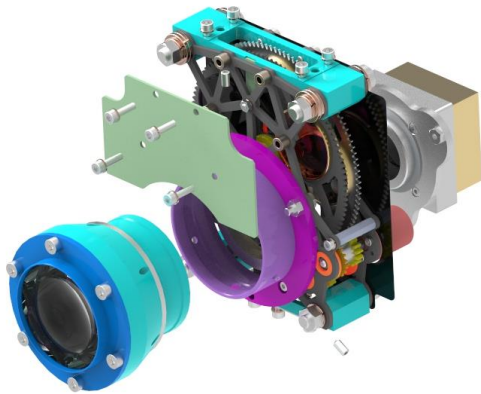


Figure 2: CAD view of the IRIS instrument without the baffle

First payload in-flight tests started as soon as the bus tests were completed. The celestial object chosen for this purpose was the galaxy of Andromeda for several reasons:

- ideal position in relation to the Moon, the Sun and the Earth ;
- low relative magnitude ;
- large apparent size ;
- high density of stars of different magnitudes around.



Figure 3: Processed image of the Andromeda galaxy captured by IRIS (visible light, no polarization, 15 s exposition time)

These first images confirmed the capacity of the instrument in terms of signal-to-noise ratio and resolution.

To demonstrate the versatility of EyeSat bus and payload, the instrument was also pointed towards the Earth. Because of the sun-synchronous orbit, the target must have been in the southern hemisphere. The lack of measurements from an Earth-directed star sensor ensured sufficient stability but degraded pointing accuracy. Thus, it was decided to target an 500 km wide area in the south of Australia.

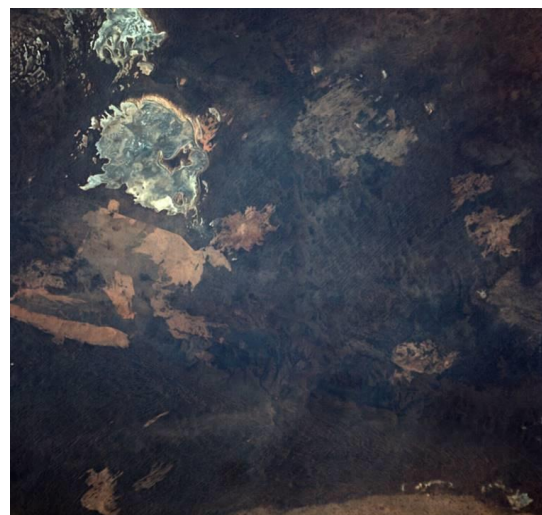


Figure 4: Processed image of Lake Maurice capture by IRIS (visible light, no polarization, 300 μ s exposition time)

The actual scene was easily identified afterwards by comparing it to known available satellite images of Australia. This is the area around Lake Maurice, Australia.

Power

Taking advantage of a 6am Sun-synchronous orbit, EyeSat's power subsystem is designed around a shunt circuit for power generation control. This fully analogical design ensures partial dissipation of power generated from solar cells through resistors on the back sides of the solar panel, when it is needed to limit battery voltage to the appropriate value. Four solar panels produce up to 24W, charging a 2S2P lithium ion 48Wh battery. Solar panels, hinges, hold-on and release mechanisms and PCBs were designed in house. The solar cells are assembled onto solar panels PCB using a home-made process that has been improved over several French CubeSat projects.

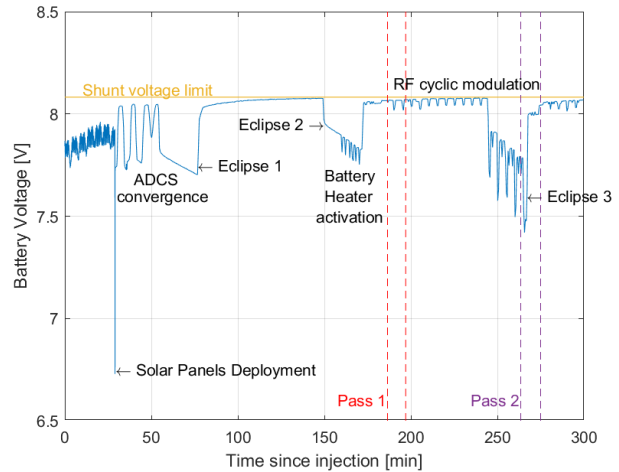
In order to limit complexity, no microcontrollers are used in the power system. It is a full sensors & actuators system. On board computer controls them via I2C and 1-Wire buses. Data are collected at different rates depending on the satellite's mode. The measurements are :

- voltage and current for each component,
- solar panels' voltage and current (post shunt),
- buses' and battery's voltage and current.

During the first hours of the satellite's life, power housekeeping data were collected and saved in the on-board computer.

During the first station pass, all telemetry since injection was downloaded to the ground, giving a clear status of the satellite at the operation center: EyeSat successfully deployed its solar panels and converged to a sun pointing. The battery was fully charged.

Just by looking at battery voltage for the five first hours post injection, we can see most of the events that occurred:



Battery Voltage over the first 5h

Analysis have been done on measurements to refine power parameters according to flight values including:

- power budget for each subsystem and mode,
- self-discharge from launch campaign to orbit injection,
- disparities between solar panels,
- shunt system performances.

Here are some comparative results between flight measurements and simulations.

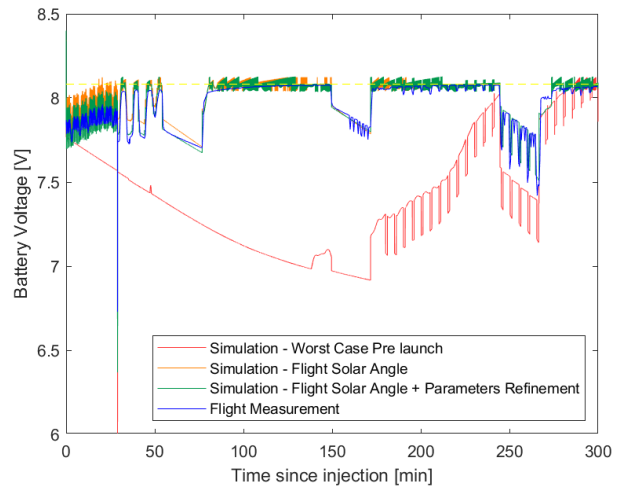


Figure 5: simulations and measurements Comparison

Results show that the worst case studied prior to launch was very conservative compared to actual flight measurements. Especially because analysis took into consideration the worst angular injection speeds.

But when the actual solar angle is used for simulation, results are highly similar to actual measurements.

Parameter adjustments described earlier improve slightly the simulation’s accuracy. Those results are very important to prove the relevance of those models that are used for sizing.

Since the LEOP phase, power housekeeping data are still collected each 30 seconds and downloaded to the ground station, being available for analysis if necessary.

Attitude Determination and Control System (ADCS)

Survival Mode

The detailed design of EyeSat’s survival mode was performed in [1].

Telemetry shows us that the convergence of the ADCS just after the orbit injection of the satellite was very fast, in particular thanks to very favorable initial kinematic conditions: the launcher put EyeSat in orbit with very low initial rotation speeds.

On the following figure, we can see some points on 12/17/2019 and a long measurement hole before resuming on 12/18/2019. This is linked to the postponement of the launch, that occurred on December 18 whereas it was expected the day before. Results are voluntarily presented as a function of the on-board time. As the launch was originally scheduled on 12/17/2019, the on-board time started at this date when the satellite was turned ON, and the jump in time comes at the moment when the on-board time was updated.

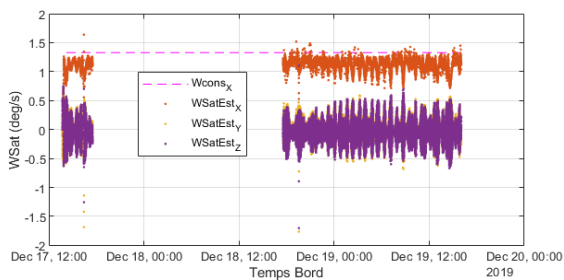


Figure 6 : Rotation rate versus on-board time

As a reminder, EyeSat’s survival mode works without solar sensors. To check its good convergence, two pieces of information are relevant:

- The current generated by solar panels: nevertheless, once the battery is full, because of the shunt dissipation system, the current can be zero although the satellite is well oriented. Thus, this observable parameter is to be handled with care, and will not be presented here.
- The measurements from the magnetometer. A good indication of the convergence state of the survival mode

is simply the measurement of the magnetic field expressed in the satellite frame. The objective of the ADCS is here to point the Xsat axis towards to the orbit’s normal direction (which turns out to be the anti-sun direction on the 6LHAN orbit). The normal to the orbit being close to the normal to the magnetic field, we must then observe that the component of the measured magnetic field is weaker along the Xsat axis with regard to the other two axes. The differentiation between the solar pointing and the anti-solar pointing, in addition to seeing whether the battery is charging or not, can be deduced from the estimated satellite’s rotation. Without going into the details of the design of survival mode [1], as long as the estimated speed is positive along Xsat, the solar panels will orient themselves towards the sun.

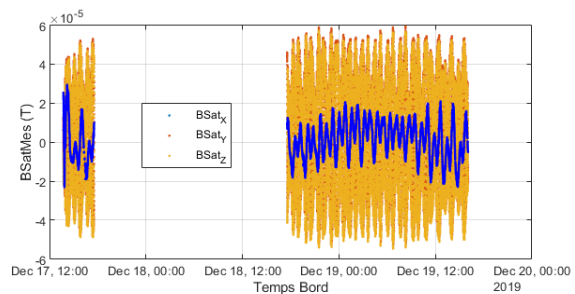


Figure 7: Magnetic field measurements

Note: Although the speed estimation is not very accurate, it can be stated here that the initial speed estimated at the time of switching on the ADCS (and therefore after the deployment of the solar panels) is around 0.15deg / s, i.e. two orders of magnitude below the values used for sizing.

Mission mode

EyeSat’s mission mode, that uses in particular four reaction wheels and a star tracker, is detailed in [2] and is divided in two sub-modes:

- The coarse pointing mode, associated to its autonomous guidance and attitude rallying module, is used for standby, downloading and maneuvers and a fine pointing mode for imaging. It works on orbit as expected with pointing accuracy around 10 degrees, which is not so bad with only a magnetometer as sensor (since the star tracker is only used in the other sub-mode).
- The fine pointing mode, upon which the satellite switches autonomously when the target pointing is inertial and the star tracker is delivering consistent measurements. Performances are detailed below.

In terms of performance evaluation, we must distinguish the attitude estimated on board by the estimation functions which represents the absolute pointing error combined with the estimation error, with the absolute

pointing error, that can be seen in the payload images. For the evaluation of the pointing stability, there are not many precise conclusions to draw from the telemetry which is sampled at a too low frequency for that purpose. On the other hand, the evaluation of the spreading of the stars on the payload images makes it possible to have a good estimate of the stability over the exposure time of the imager.

The use of images, combined with ground attitude estimation software based on starry sky images, makes it possible to estimate the bias corresponding to the misalignment between the star tracker and the payload. Once taken into account in the imaging programming, the pointing accuracy is significantly improved.

An illustration is provided below. A first image of the Andromeda constellation was taken on December 31, and a reduced size image was downloaded (1000 pixels x 1000 pixels out of the possible 2048 x 2048). The target is circled in red, and it can be seen that it is not perfectly centered.

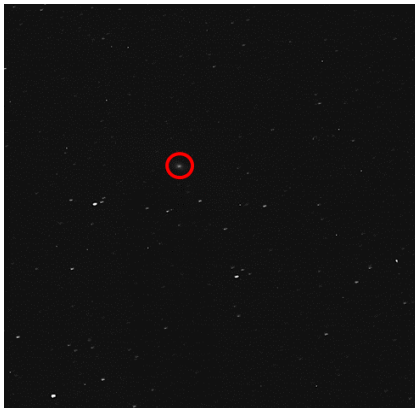


Figure 8: first picture of Andromeda

Ground processing, based on an identification of the stars present on the image, makes it possible to estimate a bias of approximately 1 degree between the target attitude and the attitude corresponding to this image.

A new image was taken on January 9, 2020, taking into account the estimated bias. On the new image, from which all the pixels were downloaded, the target is better centered.

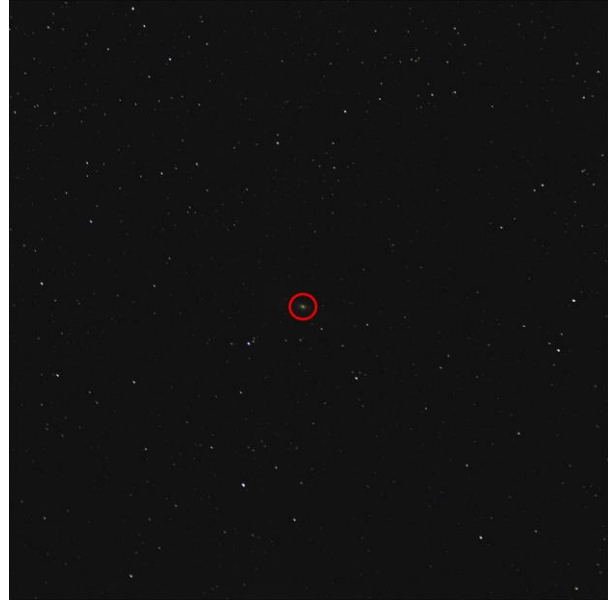


Figure 9: second picture of Andromeda

Here is a realistic evaluation of the maximum absolute pointing errors, performed by EyeSat in fine pointing mode, after calibration.

	Around Xsat	Around Ysat or Zsat
Estimated error	1370 μ rad	830 μ rad
Accuracy of the estimation	450 μ rad	150 μ rad
Residual biases	800 μ rad	800 μ rad
Total : Absolute error (quadratic sum of the different contributors)	1650 μ rad 0,09 deg	1160 μ rad 0.07 deg

As said before, stability can be evaluated thanks to payload's image processing, allowing us to estimate the shaking during the exposure time. Results show a stability of 880 μ rad (0.05 degrees) over 15 seconds.

Thermal control

The thermal control subsystem is composed of:

- Secondary Surface Mirrors (SSM) to dissipate heat,
- Multi-Layer Isolation (MLI) sheets,
- active control with one heater on the battery pack and one heater on the star tracker.

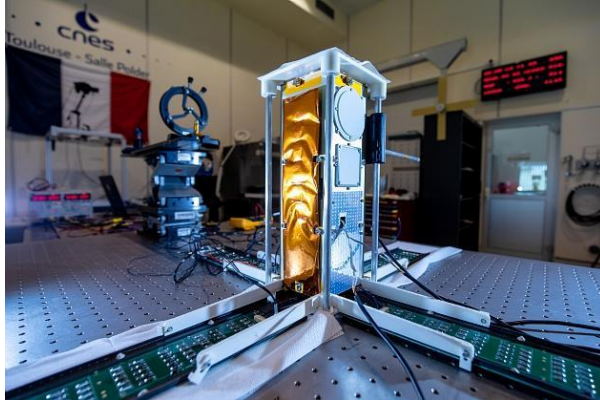


Figure 10: EyeSat flight model in clean room. MLI and SSM are visible.

The goal is to maintain all the subsystems' temperatures within their operational range. Since every part of the satellite is conductively coupled with the structure, the interior temperature is quite homogeneous. Therefore, the design of the thermal control subsystem is driven by the most restrictive temperature range, which is the batteries' (0°C to 40°C).

Temperatures were predicted with SYSTEMA / THERMICA. The numerical model results were first compared with the data acquired during thermal vacuum testing on the qualification model and on the flight model. Based on those comparisons, the model has been rectified so that the results it gives match as best as possible the real data.

The pictures below show the temperature variation of some electronic components over several orbits. The first one plots housekeeping data whereas the second one comes from simulation.

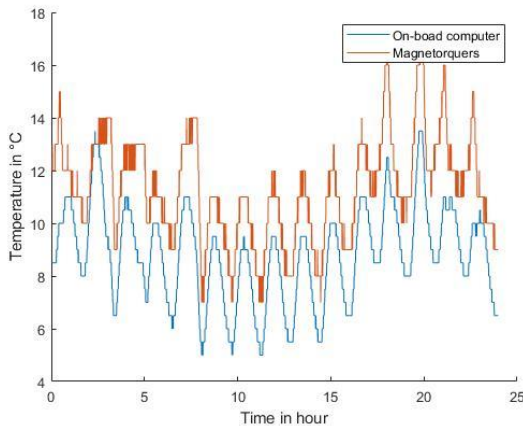


Figure 11: In-orbit electronic components' temperatures (01/01/2020)

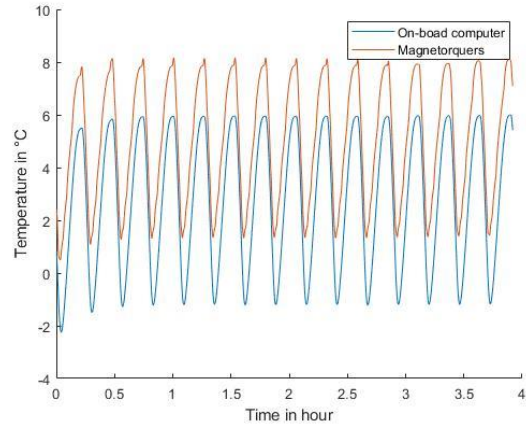


Figure 12: Electronic components' temperature predictions

The mean difference of 6°C between prediction and reality is quite good.

The pictures below show the temperature variation of the solar arrays over several orbits.

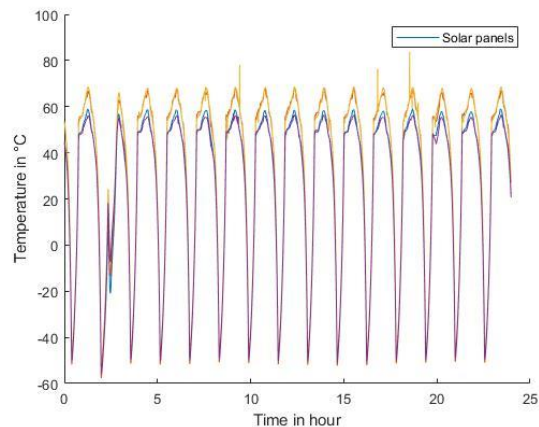


Figure 13: In-orbit solar arrays' temperature (01/01/2020)

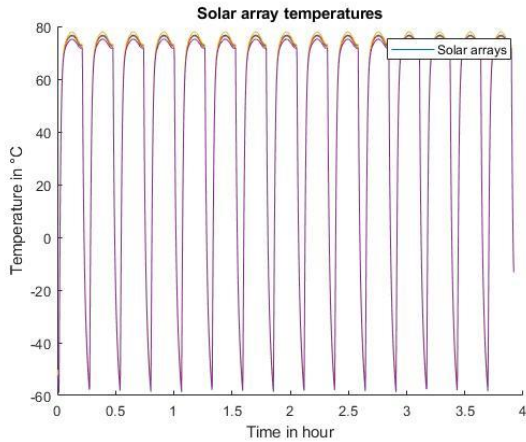


Figure 14: Solar arrays' temperature predictions

The prediction is slightly more conservative with a maximum temperature of almost 80°C and a minimum temperature of -60°C whereas in-orbit data show a variation between 70°C and -50°C. Again the simulation is very close to reality.

The graph below shows the batteries' temperature and the heater's duty cycle. The target temperature range is 10°C to 14°C. The control of this temperature is well ensured.

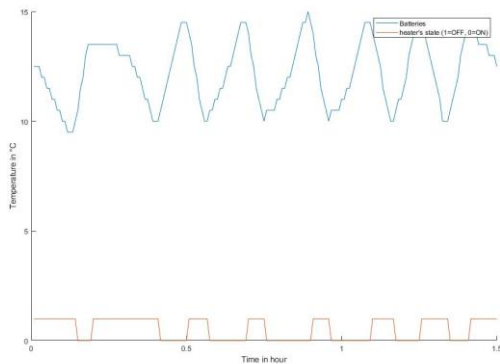


Figure 15: In-orbit batteries' temperature (01/01/2020)

The last comparison concerns the camera's temperature. The two graphs below show in-orbit data and predictions. There is a mean difference of 6°C as observed for the on-board computer and the magnetorquers.

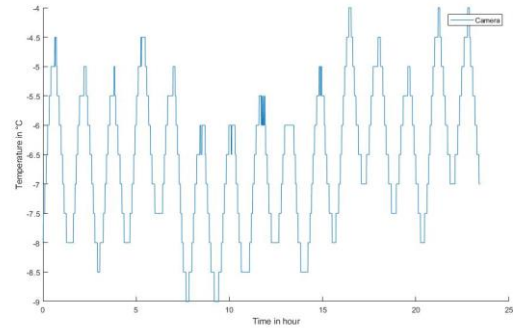


Figure 16: In-orbit camera's temperature (01/01/2020)

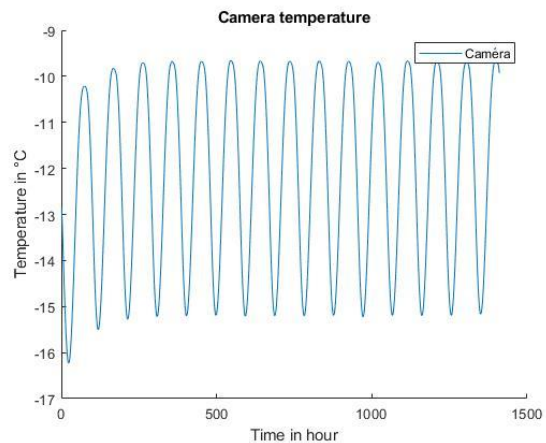


Figure 17: camera's temperature predictions

Flight Software

EyeSat's flight software is based on a Time and Space Partitioning architecture using FentISS hypervisor XtratuM and real-time OS LithOS. The flight software is thus divided into several partitions whose execution is managed by the hypervisor that statically allocates them CPU time and memory area. Among these partitions, three are called Basic SoftWare (BSW) and provided by the framework LVCUGEN developed by CNES. These partitions are generic, configurable and tunable through static or dynamic configuration tables and drivers. They fulfill three main functionalities:

- memory and mode management ;
- hardware and software error management ;
- input and output management.

Most of the other partitions are bus specific partitions. Each partition manage a functional chain of the spacecraft:

- Control & Command ;

- Guidance, Navigation and Control ;
- Thermal Control System ;
- Communications.

Eventually the last partition is mission specific. It deals with payload management.

In order to mitigate the risk of corruption of the working data, the error correction codes (ECC) capability is activated in the main RAM memory. This mechanism is able to restore the original information when reading a word that has suffered a single bit-flip. In order to stimulate that mechanism, a continuous background scrubbing is performed on most of the RAM memory (with the notable exception of the area where the hypervisor itself resides). The scrubbing task simply periodically reads the words one by one, in order to trigger bit-flips corrections when needed.

The adopted design demonstrated a good reliability over the course of the first 5 months of the mission, given that only one occurrence of the flight software crashing could be observed. Whereas it is difficult to provide a definitive conclusion regarding the cause of the crash, a Single Event Upset (SEU) due to exposure to space environment is held as the most probable cause.

Regarding storage, a 16 GB NAND flash memory is used as non-volatile storage for:

- flight software executable files (including FPGA configuration file) ;
- context elements (on-board time, TMs) ;
- payload-related storage (pictures).

Due to the unreliable nature of NAND flash memory, specific measures were implemented to ensure the integrity of data, most importantly of the flight software files. Indeed each file is triplicated, and a majority vote is performed on each 4 bytes word by the boot loader, so that the correct file can be rebuilt in the presence of corruption in the individual copies.

This mechanism proved useful as corruptions were detected by the boot loader in one of the FPGA configuration files (bitstreams), first in one of the copies, then two, then all three of them; despite all this, the boot loader always succeeded to rebuild the original file. An investigation to determine the extent of the corruptions has yet to be conducted.

On top of that, 3 independent copies of the flight software are stored on board. This is *not* to provide any kind of data integrity, but rather to ensure the safety of the in-flight software update process. 2 copies are designated as *current* flight software, so that one of them is the currently running version, and the other one is

available for upload. The 2nd copy is labeled *recovery*, and serves as a backup in case of corruption during the upload process.

This update process has been successfully used twice in the early phases of the mission.

OPERATIONS

Eye-Sat uses a modern control center called SCC : Simple Control Center. SCC uses modern software technologies : Dropwizard, microservices, Angular. A good synopsis for this tool would be to say that it has a light installation manual, a light user manual and great graphics user interface.



Simple Control Center uses a procedure language tool in order to enhance engineers' work. This tool is highly inspired from the Spell reference language and is compatible with it. It is actually a groovy implementation of the Spell Reference Language to which new features have been added such as: auto-completion, automatic mapping from XTCE (CCSDS system database standard). By design the tool takes advantage of all the groovy language's power which is itself a java extension. And so it is fully compatible with java which has already a very rich scientific library ecosystem. This procedure language enables operators to automate flight software validation, system validation, and moreover operations.

Operations are based on routines developed in groovy and previously tested on the satellite qualification model. These routines run automatically at each station pass. The typical sequence consists of downloading the observables, correcting the on-board time, programming the transmitter for the next passes and then programming the mission plan. The interface with the rest of the ground segment and the mission center is based on the exchange of xml files.

U-SPACE

From academia and research to industry, U-Space illustrates how student projects can lead to successful start-ups. This private company was founded by former EyeSat interns. U-Space designs, builds and operates high-performance nanosatellites that address a large variety of missions. Its teams leverages several years of experience spent at CNES and leads space projects from the early stages of development up to launch and operations.

ACKNOWLEDGMENTS

The EyeSat Project would like to thank all the people and organizations who made this wonderful project possible. In particular, we would like to thank:

- the 250+ students who worked on the project,
- CNES and all the people involved,
- the academic partners : ISAE-SUPAERO, ENAC and IUT of Cachan,
- all the industrial partners.

With the results obtained, the objectives of the project are fulfilled.

REFERENCES

1. Viaud F., Lagrange O., Safe Mode Attitude Control Of EyeSat Mission, EuroGNC 2017, Warsaw, Poland, 2017.
2. Viaud F., and al, Flight Dynamics for the Astronomy Mission EyeSat, The 4S Symposium 2018, Sorrento, Italia, 2018.
3. Apper F., and al, Eye-Sat: A 3U student CubeSat from CNES packed with technology, 33th annual small satellite conference, Logan, Utah, USA, 2019.
4. Gaboriaud A., JANUS a CNES (French Space Agency) Program for Developing Cubesats by Students, 31st annual small satellite conference, Logan, Utah, USA, 2017.
5. Levasseur-Regourd A.C. & al., Eye-Sat, a triple Cubesat to monitor the zodiacal light intensity and polarization, European Planetary Science Congress, Cascais, Portugal, 2014.
6. Issler J.L. & al, "CCSDS Communication products in S and X band for CubeSats", AIAA Small Satellites Conference, Utah State University, USA, 2014.
7. Humeau N. and Gateau T., A Lightweight and Efficient Control Center Based on Modern technologies, SpaceOps 2018.